Biophysical Chemistry 173–174 (2013) 8–14

Contents lists available at SciVerse ScienceDirect

Biophysical Chemistry

journal homepage: http://www.elsevier.com/locate/biophyschem

His–Trp cation–π interaction and its structural role in an α-helical dimer of HIV-1 Vpr protein

Takayuki Kamiyama, Takashi Miura, Hideo Takeuchi *

Graduate School of Pharmaceutical Sciences, Tohoku University, Aobayama, Sendai 980-8578, Japan

HIGHLIGHTS

- The H_{III} region of HIV-1 Vpr protein forms an antiparallel dimer.
- Protonation of His71 induces a cation–π interaction between His71 and Trp54.
- The cation–π interaction elongates the helix and increases the dimer stability.
- The dimeric structure is modified to a more compact form by the cation–π interaction.

GRAPHICAL ABSTRACT

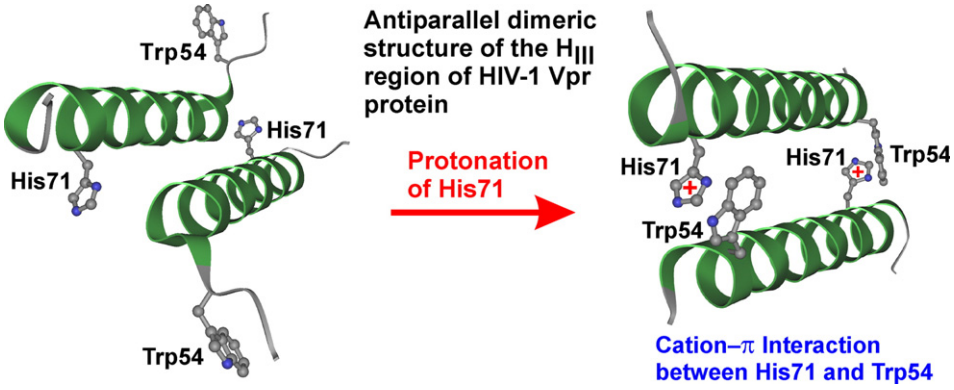

ARTICLE INFO

Article history:
Received 28 December 2012
Received in revised form 22 January 2013
Accepted 26 January 2013
Available online 14 February 2013

Keywords:
HIV-1
Vpr protein
Cation–π interaction
Fluorescence
Circular dichroism
UV absorption

ABSTRACT

Vpr is a multifunctional accessory protein of HIV-1 virus and was previously proposed to assume an antiparallel helical dimer with the third helices H_{III} of different subunits facing each other. In this study, we have examined the structure and stability of the antiparallel dimer by using a fragment peptide, Vpr52–80, spanning the H_{III} region. The present analyses of fluorescence, circular dichroism, and UV absorption spectra have shown that a cation–π interaction takes place between protonated His71 and Trp54 located near the opposite ends of the two antiparallel helices. The cation–π interaction induces a small elongation of the H_{III} helix, an increase in thermal stability of the helical dimer, and a modification of the helix arrangement to produce a more compact form. The His71–Trp54 cation–π interaction may be utilized in stabilizing and tuning the dimeric structure of Vpr to achieve proper interactions with other proteins.

1. Introduction

Human immunodeficiency virus type 1 (HIV-1) is a highly infective retrovirus that causes acquired immunodeficiency syndrome (AIDS) [1]. The genome of HIV-1 encodes several accessory proteins that are not necessary for in vitro replication of the virus but are required for in vivo replication, dissemination, and persistence [2–4]. The viral protein R (Vpr) is one of such accessory proteins and has been implicated in many processes of the virus life cycle, contributing to the high morbidity and mortality of AIDS [5–7]. The multifunctional nature of Vpr is believed to arise from its interactions with a variety of viral and

* Corresponding author. Tel./fax: +81 22 795 6855.
E-mail address: takeuchi@m.tohoku.ac.jp (H. Takeuchi).

0301-4622/$ – see front matter © 2013 Elsevier B.V. All rights reserved.
http://dx.doi.org/10.1016/j.bpc.2013.01.004

host cellular proteins [6–9], though the mechanisms of interactions in individual processes are poorly understood. Investigation of structural characteristics of Vpr may provide important clues to how Vpr interacts with other proteins to perform its functions.

Vpr is a relatively small protein composed of 96 amino acid residues [10,11]. The secondary and higher-order structures of Vpr have been investigated by nuclear magnetic resonance (NMR), circular dichroism (CD), and fluorescence spectroscopy [12–19]. According to NMR studies on the full-length Vpr protein dissolved in acidic aqueous-organic solvents, Vpr folds into three amphiphilic helices (H_I, Asp17–Phe34; H_{II}, Trp38–Tyr50; H_{III}, Thr53–His78) in the central region of the polypeptide chain (Fig. 1A) [16,18]. Another NMR study on a C-terminal fragment (Vpr52–96) at pH 3 in the presence of 30% acetonitrile has shown that the fragment peptide forms a dimer, in which the H_{III} helices (Thr53–Gly75 in this case) of different two peptide molecules face each other in a nearly antiparallel orientation (Fig. 1B) [19]. The main part of the dimeric interface is a Leu-zipper-like motif composed of four hydrophobic residues (Vla57, Ile61, Leu64, and Leu68) aligned on one side of each helix. Near the helical ends, on the other hand, Trp54 of one helix is close to His71 of the other oppositely oriented helix, suggesting an interaction between them. Trp54 and His71 as well as the hydrophobic residues involved in the H_{III} dimerization are highly conserved in Vpr mutants found in AIDS patients [20,21], implying biological relevance of the H_{III} dimerization.

The imidazole ring of His can be protonated to be cationic at acidic pH with an average pK_a value of 6.6 ± 1.0 in proteins [22]. On the other hand, the π-electron-rich indole ring of Trp attracts a nearby cation through the so-called cation–π interaction, which is increasingly recognized as an important electrostatic interaction in structural formation and functioning of proteins [23–27]. Thus, the close proximity of Trp54 and His71 in the NMR dimeric structure of Vpr raises the possibility that a cation–π interaction occurs between His71 and Trp54, and the interaction contributes to the dimer formation of Vpr. Dimers and trimers of Vpr have been found in the cytoplasm and nucleus of HIV-1-infected cells [28], and oligomerization of Vpr has been proposed to be an essential feature for its function [29].

In this study, we have investigated the possibility of cation–π interaction between His71 and Trp54 by using a fragment peptide of Vpr containing the H_{III} region. Fluorescence, CD, and UV absorption spectra of the model peptide were examined in organic solvent-free aqueous solutions not only at acidic pH but also at neutral pH, and in some cases, at varied temperatures. Comparison of the spectra at different pH and temperatures has shown that the cation–π interaction between His71 and Trp54 really occurs at pH<5.5, inducing a little elongation of the H_{III} helix, an increase in thermal stability of the helical dimer structure, and a modification of the helical arrangement. The His71–Trp54 cation–π interaction is likely to play a role in stabilizing and tuning the dimeric structure of Vpr to achieve proper interactions with various kinds of viral and cellular proteins.

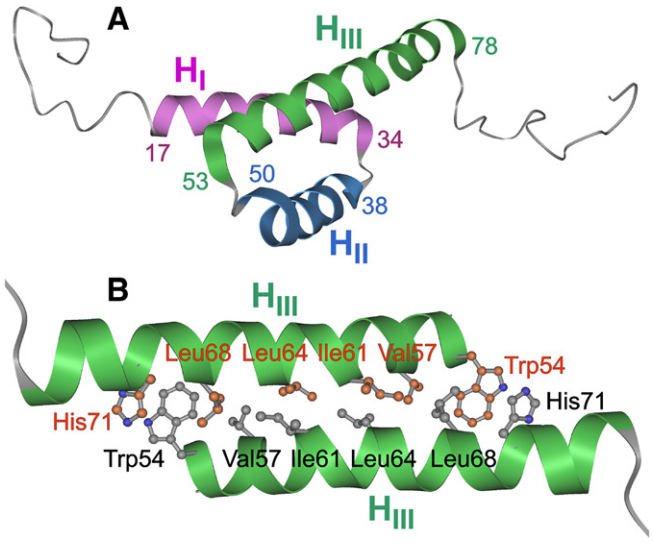

Fig. 1. Structures of (A) full-length Vpr and (B) a dimer of Vpr52–90 in water/acetonitrile (70/30) solution (pH 3.0) determined by NMR spectroscopy [18,19]. The atomic coordinates were taken from Protein Data Bank (codes 1M8L and 1X9V). The first and last residues of helices H_I, H_{II}, and H_{III} are shown for full-length Vpr. For the dimer of Vpr52–90, residues located in the interface of two H_{III} helices are indicated. The carbon atoms and name labels of the residues belonging to the helix on the far side are colored in orange.

2. Materials and methods

2.1. Materials

The 29-mer peptide Vpr52–80 ($D^{52}TW^{54}TGVEALIRILQQLLFIH^{71}FRIGCRHSR^{80}$) and its His71 → Ala (H71A) mutant were synthesized on an automated peptide synthesizer (Applied Biosystems, model 431A) by using standard Fast Moc chemistry. To cleave any disulfide bonds involving the Cys76 side-chain, the crude peptide was reduced with 50 molar equivalent of dithiothreitol at 40 °C and at neutral pH for 1 h. After the reduction, the solution was acidified with trifluoroacetic acid (TFA) and subjected to HPLC purification on a reversed-phase column (Cosmosil $5C_{18}$-AR300) using a gradient mobile phase of aqueous methanol (30–70%) containing 0.1% (v/v) TFA. The purified peptide was dissolved in 0.1 M HCl and then lyophilized for conversion to hydrochloride salt. The N- and C-termini of the synthesized peptides were capped with acetyl and amide groups, respectively, to mimic the preceding and following peptide bonds within the full-length protein.

8-Anilino-1-naphthalenesulfonic acid (ANS), which serves as a fluorescent probe of surface hydrophobic regions of peptides and proteins [30,31], was purchased from Sigma-Aldrich and used as received.

2.2. Fluorescence, CD, and UV absorption spectra

Samples for spectral measurements were prepared as follows. Lyophilized powder of Vpr52–80 or its H71A mutant was dissolved in 1 mM glycylglycine and the solution was subjected to fluorescence and CD spectral analysis. For UV absorption measurements, the peptide was dissolved in deionized H_2O without glycylglycine to avoid interference from the buffer UV absorption. For every peptide solution, the peptide concentration was 20 μM and the pH was adjusted by adding aliquots of 0.1 M HCl or NaOH. The peptide concentration was determined from the UV absorption intensity of Trp54 at 280 nm ($\varepsilon_{280} = 5500\ M^{-1}\ cm^{-1}$) [32]. Binding of the hydrophobic probe ANS to the peptide was examined by fluorescence spectroscopy for a mixture of 10 μM ANS and 20 μM Vpr52–80 in 1 mM glycylglycine buffer. The ASN concentration was determined by weight.

Fluorescence spectra were recorded on a Jasco FP-6500 spectrofluorometer with a 3 mm × 3 mm quartz cell. The fluorescence emission from Trp54 was excited at 280 nm and that from ANS was excited at 370 nm. The intensities of fluorescence measured on different days were calibrated with the Raman scattering from solvent H_2O, which appeared at 309 nm when excited at 280 nm. CD spectra were recorded on a Jasco J-820 spectropolarimeter with a quartz cell of 1 mm path length and the spectra were averaged over four scans. The observed ellipticity was converted to mean residue molar ellipticity. To evaluate the secondary structure contents from the observed CD spectra, the computer program CDSSTR in the CDPro package was used [33]. UV absorption spectra were recorded on a Hitachi U-3300 spectrophotometer with a 3 mm quartz cell. The background signals due to solvent were subtracted from the sample fluorescence, CD, and UV absorption spectra. The temperature of the sample cell was controlled using a water jacket connected to a constant-temperature circulating bath. The reproducibility of the spectral data was confirmed by two or more

independent measurements and the standard deviations of plotted points were estimated to be less than the sizes of the data point symbols.

3. Results

3.1. pH-dependence of the Trp54 fluorescence intensity

Fig. 2A shows the fluorescence spectra of wild-type (WT) Vpr52–80 observed at pH 3.5–7.3 with excitation at 280 nm. The fluorescence band at 345 nm is ascribed to Trp54, the unique Trp residue of Vpr52–80 [34]. Although the pH of the sample does not significantly affect the fluorescence peak wavelength, the fluorescence intensity decreases by about 70% on going from pH 7.3 to 3.5 (Fig. 2A). Analogous quenching of Trp fluorescence at acidic pH was previously reported for a longer Vpr peptide, Vpr52–96 [19]. To further examine the pH dependence of fluorescence intensity, the peak intensity at 345 nm was plotted against pH in Fig. 2C (circle). Analysis of the sigmoidal intensity change using a Hill equation gave a pK_a value of 5.5 ± 0.1 and a Hill coefficient close to unity (1.1 ± 0.1) [35]. The obtained pK_a and Hill coefficient suggest that Trp54 interacts with a nearby chemical group that undergoes protonation at pH 5.5 without mutual interactions among the groups of the same type. Furthermore, the significantly diminished fluorescence at pH<5.5 indicates that the chemical group acts as a strong quencher of Trp fluorescence only in its protonated form.

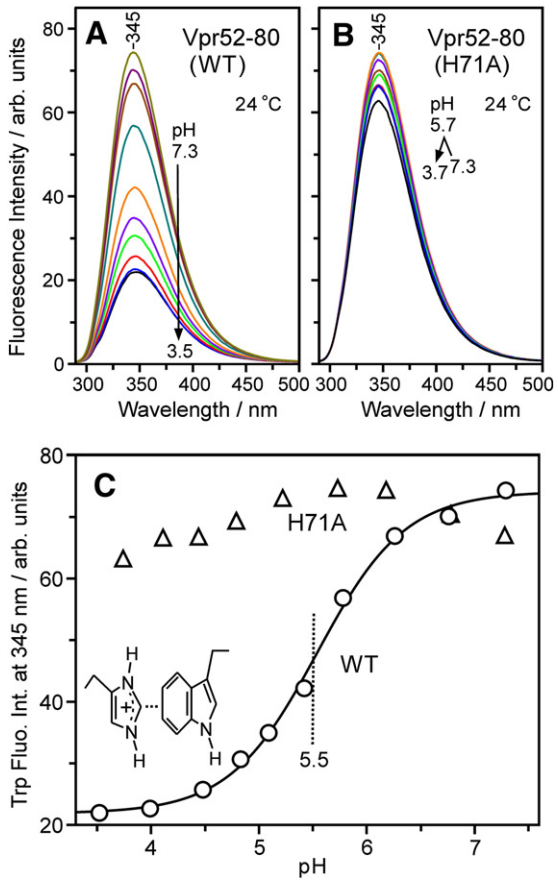

Fig. 2. Trp fluorescence spectra of (A) wild-type Vpr52–80 and (B) its H71A mutant at 24 °C and at varied pH. The peptide concentration was 20 μM and the spectra were excited at 280 nm. The spectral change associated with the pH change is indicated with an arrow (pH 7.3–3.5 for A) or a bent arrow (pH 7.3–5.7–3.7 for B). The fluorescence intensity at 345 nm is plotted against pH in C for the wild type (circle) and the H71A mutant (triangle). The transition at pH 5.5 observed for the wild type is indicated with a dotted vertical bar. A model of cation–π interaction between protonated His and Trp is depicted in the inset of C.

Of the amino acid residues composing Vpr52–80, the side-chains of Asp52, Glu58, His71, Cys76, and His78 can be protonated at acidic pH [22]. Since the fluorescence of Trp is quenched by amino acids such as Asp, Glu, His, and Cys [34], all of the residues listed above are candidates for the quencher of Trp54 fluorescence. Among them, His71 is the most likely candidate because His71 is located close to Trp54 in the dimeric structure of Vpr52–96 proposed by NMR [19]. To decide whether His71 is really the quencher of Trp54 fluorescence, we prepared the H71A mutant of Vpr52–80 and recorded its fluorescence spectra at pH 3.7–7.3 (Fig. 2B). In contrast to the WT peptide, the H71A mutant exhibits little pH dependence and no significant quenching occurs around pH 5.5 (Fig. 2C, triangle). This observation clearly indicates that His71 is responsible for the quenching of Trp54 fluorescence of WT Vpr52–80 at pH<5.5. At pH<5.5, His71 may be protonated at both nitrogen atoms of the imidazole side-chain and the protonated imidazole (cationic imidazolium) ring of His71 quenches the fluorescence of Trp54. The close link between the His71 protonation and the Trp54 fluorescence quenching is consistent with the literature report that the cationic form of His quenches Trp fluorescence much more efficiently than the neutral form if both residues are in close proximity to each other [36,37]. It is very likely that protonated (cationic) His71 is located near Trp54 (of the same or a different peptide chain) at pH<5.5, and an interaction between these two residues causes the fluorescence quenching as illustrated in Fig. 2C.

3.2. His71–Trp54 cation–π interaction as revealed by UV absorption

To further investigate the nature of interaction between Trp54 and His71 at pH<5.5, we examined the pH dependence of UV absorption. In a previous paper [25], we showed that the B_b absorption of the Trp indole ring around 220 nm slightly weakens and shifts to the red when a K^+ ion electrostatically interacts with the π-electrons of the indole ring. Analogous weakening of the B_b absorption accompanied by a red shift was observed for other cation–Trp pairs and is now regarded as a decisive marker of cation–π interaction of Trp [26,27]. Fig. 3 compares UV absorption spectra of WT Vpr52–80 below (pH 4.8) and above (pH 7.3) the transition pH (5.5) of fluorescence quenching. The difference between the two spectra is small but significant as demonstrated in the difference spectrum (pH 4.8 *minus* pH 7.3) expanded by a factor of five (bottom trace in Fig. 3). Although the change of B_b absorption is seen on a gently sloping background reflecting a change in main-chain amide absorption, a weak positive peak at 231 nm and a stronger negative peak at 222 nm are evident. The negative–positive peak pair at 222/231 nm is very similar to

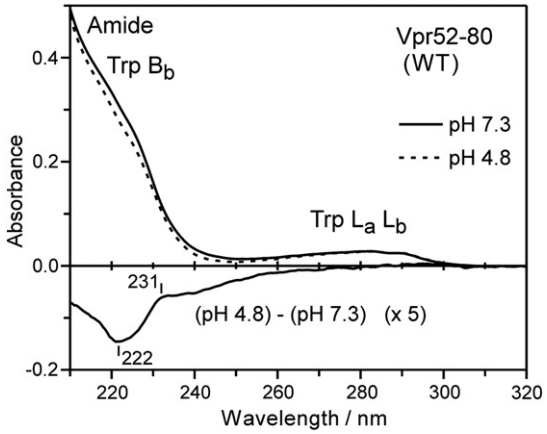

Fig. 3. UV absorption spectra of wild-type Vpr52–80 (20 μM) at pH 4.8 and 7.3. The difference, pH 4.8 *minus* pH 7.3, expanded five-fold is also shown in the bottom trace. The weak absorption in the 260–300 nm region is assigned to the L_a and L_b transitions of Trp indole ring. The strong absorption around 220 nm is ascribed to the Trp B_b transition, while a very strong absorption due to the main-chain amide tails up to about 260 nm.

those reported previously for Trp residues involved in cation–π interactions [26,27]. This observation gives evidence that the His71–Trp54 interaction detected in the form of fluorescence quenching at pH<5.5 (Fig. 2) is really a cation–π interaction. Although fluorescence quenching can occur by a number of different mechanisms [38], UV absorption spectroscopy provides a clue to the identification of the quenching induced by cation–π interaction.

3.3. Helical structure and its pH-dependent elongation

To obtain further information on the structure of Vpr52–80, the pH dependence of the secondary structure of this peptide was examined by CD spectroscopy. Fig. 4 compares the CD spectra of WT Vpr52–80 at pH 4.1, 5.7, and 7.4. These spectra exhibit three isodichroic points at 198, 210, and 221 nm (crossing points of the spectral curves in Fig. 4), suggesting the presence of a two-state structural transition between pH 4.1 and 7.4. To analyze the transition in terms of secondary structure content, the CD spectra including those recorded at other pH values were processed with the computer program CDSSTR of the CDPro package [33]. The percentages of α-helix, β-sheet, turn, and irregular structure predicted by CDSSTR are plotted against pH in the inset of Fig. 4. The α-helical content is much higher than those of the other structures throughout a pH range of 4–7.5, indicating that Vpr52–80 is predominantly α-helical in nature and serves as a good model for the H_{III} region of Vpr.

According to the dimeric structure of Vpr52–96 determined by NMR at pH 3.0 [19], the H_{III} helix is localized in the N-terminal region (Thr53–Gly75) with the C-terminal tail (Cys76–Ser96) being in irregular structure (Fig. 1). If the NMR structure of Vpr52–96 applies to Vpr52–80 at pH<5.5, the Thr53–Gly75 region (23 residues) is folded into an α-helix corresponding to H_{III}, while the N-terminal Cys76–Arg80 region assumes an irregular structure. This structural model of Vpr52–80 contains 23 α-helical residues within 29 total residues (~80%) and is consistent with the high α-helical content (~85% at pH<5.5) revealed by CD spectroscopy (Fig. 4). In the highly α-helical structure of Vpr52–80, Trp54 and His71 of the same peptide molecule are located far away from each other on one α-helix, and the interaction between them is impossible to take place. However, if we assume an antiparallel dimeric structure of Vpr52–80 as proposed by NMR for Vpr52–96 [19], His71 is enabled to interact with Trp54 of another peptide molecule. In other words, the presence of the His71–Tp54 cation–π interaction gives support for an antiparallel helical dimer structure of Vpr52–80. The antiparallel helical arrangement of two peptide units may be the fundamental structural feature of Vpr.

The secondary structure of Vpr52–80 shows a small but significant change at pH 5.5 (inset of Fig. 4). The α-helical content is a little higher at pH<5.5 than at pH>5.5 with an opposite change of the irregular structure content at the same pH (Fig. 4, inset), suggesting a conformational change from irregular to α-helical upon decrease of pH below 5.5. Generally, a conformational transition from irregular to α-helical is expected to increase the hypochromism of the peptide main-chain UV absorption [39]. Actually, the UV absorption difference spectrum in Fig. 3 has revealed a gently sloping negative background ascribable to a decrease of the peptide main-chain absorption at acidic pH, being consistent with the α-helical elongation. Furthermore, the pH of α-helical elongation well corresponds to the pH of onset of the His71–Trp54 cation–π interaction revealed by florescence spectroscopy (Fig. 2). The coincidence of the transition pH may not be accidental but would suggest a correlation between the α-helical elongation and cation–π interaction. Probably, a few residues including Trp54 and/or His71 near the C- and/or N-terminal ends of H_{III} are in irregular structure above pH 5.5 but they fold into α-helical structure below pH 5.5 to elongate the H_{III} helix with the help of cation–π interaction between His71 and Trp54.

3.4. Contribution of the cation–π interaction to the stability of helical dimer

The stability of the antiparallel helical dimer structure of Vpr52–80 was investigated by CD spectral measurements at varied temperatures. Fig. 5 shows the temperature dependence of the ratio of molar ellipticities at 208/215 nm ($[\theta]_{208}/[\theta]_{215}$), which is sensitive to pH and serves as a marker of the secondary structure transition (Fig. 4). The $[\theta]_{208}/[\theta]_{215}$ ratio is nearly constant around 1.1 below 30 °C, while it decreases significantly at higher temperatures. The temperature dependence is well approximated with a sigmoidal curve as shown in Fig. 5 [40]. The inflection point of the sigmoidal curve is seen at 49 °C for the sample at pH 7.3, while it shifts up to 54 °C for the sample at pH 4.8. The elevated transition temperature at pH 4.8 clearly indicates that the His71–Trp54 cation–π interaction between two H_{III} helices contributes to the stabilization of the H_{III} helical dimer structure. Once the helical dimer structure is partially destroyed at higher temperatures, positively charged His71 seems to further destabilize the helical structure because the drop of the $[\theta]_{208}/[\theta]_{215}$ ratio above the transition temperature is larger at pH 4.8 than at pH 7.4. The His71–Trp54 cation–π interaction may be a key force that enhances thermal stability of the helical dimer at acidic pH.

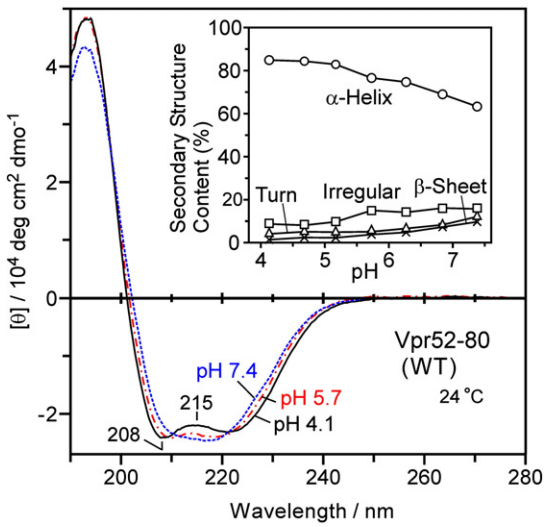

Fig. 4. CD spectra of wild-type Vpr52–80 (20 μM) at pH 4.1, 5.7, and 7.4. The spectra were recorded at 24 °C. Three isodichroic points are seen at 198, 210, and 221 nm. The inset shows the percentage contents of α-helix (circle), β-sheet (cross), turn (triangle), and irregular structure (square) obtained by using the computer program CDSSTR in the CDPro package [33].

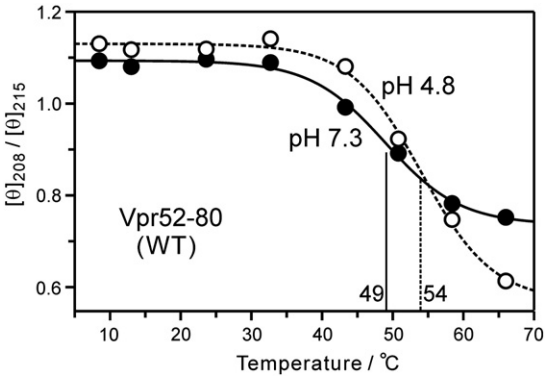

Fig. 5. Temperature dependence of the CD spectrum of wild-type Vpr52–80 (20 μM) at pH 4.8 and 7.3 as monitored by using the ratio of molar ellipticities at 208 and 215 nm ($[\theta]_{208}/[\theta]_{215}$, see Fig. 4). The solid and dotted vertical bars at 49 and 54 °C indicate the temperature of transition midpoint for pH 7.3 (closed circle) and 4.8 (open circle), respectively.

3.5. Environmental fluctuation of Trp54 diminished by the cation–π interaction

The intensity of Trp fluorescence generally decreases with increase of temperature as a consequence of non-radiative deactivation of the excited electronic state by environmental thermal fluctuations [41]. Such thermal quenching may be used as a probe of the dynamical mobility of protein structures surrounding Trp residues [41,42]. Fig. 6 shows the temperature dependence of Trp fluorescence intensity for WT (open circle) and H71A (triangle) of Vpr52–80 at pH 3.7. The data for WT Vpr52–80 at pH 7.3 (closed circle) and amino acid Trp at pH 3.7 (cross) are also shown for comparison. The fluorescence peak intensities observed at varied temperatures are normalized to that at the lowest temperature (5 °C). As seen in the figure, the Trp fluorescence intensity generally decreases with increase of the temperature and the slope of the decrease is regarded as a measure of the degree of thermal quenching. The largest quenching slope is seen for amino acid Trp, which is deactivated by collisions with thermally agitated solvent water molecules. On the other hand, Trp54 of Vpr52–80 is less quenched than amino acid Trp, reflecting a partially protected environment within the peptide structure. The smallest thermal quenching is observed for WT Vpr52–80 at pH 3.7, whereas the peptide having neutral His71 (WT, pH 7.3) or lacking His71 (H71A, pH 3.7) shows a medium thermal quenching. This observation clearly indicates that protonated His71 plays an important role in reducing the fluctuation of the peptide structure around Trp54 through the His71–Trp54 cation–π interaction. The hump around 55 °C in the fluorescence decay curve of WT Vpr52–80 at pH 3.7 may be ascribed to the loss of the cation–π interaction, which is another factor that quenches Trp fluorescence.

3.6. Modification of helical dimer structure by the cation–π interaction

ANS is a small dye molecule that has been widely used as an extrinsic fluorescence probe of protein structure [30,31]. The dye is minimally fluorescent in aqueous solution but exhibits a strong fluorescence when bound to proteins. The binding of ANS to proteins is driven by hydrophobic and electrostatic interactions [31,43]. The hydrophobic interaction occurs between aromatic rings of ANS and hydrophobic regions of proteins (see Fig. 7A for the molecular structure of ANS). On the other hand, the electrostatic interaction occurs between the negatively charged sulfonate group of ANS and positively charged amino acid side-chains [44]. Although ANS binds to proteins through hydrophobic and electrostatic interactions, the ANS fluorescence intensity may be used as a probe of surface-accessible hydrophobic regions of proteins because ANS emits much stronger fluorescence in non-polar hydrophobic environment than in polar environment [43].

Fig. 7 shows florescence spectra of ANS (10 μM) in the presence of 20 μM WT Vpr52–80 (A) or its H71A mutant (B) at pH 3.7 and at 5–69 °C. The spectra were recorded at the same pH (3.7) to avoid the pH-dependent residue ionization that might affect electrostatic binding of ANS. The peak of the ANS fluorescence is observed at 469 nm in the presence of the H71A mutant, while it decreases to 464 nm in the presence of WT Vpr52–80. The 5-nm blue shift suggests that the environment of ANS is less polar when bound to the WT peptide than to the H71A peptide [43].

The peak intensity of ANS florescence in the presence of peptide is plotted against temperature in Fig. 7C together with that of free ANS. Unbound ANS in polar environment gives negligibly weak fluorescence and therefore the fluorescence intensity in the presence of peptide straightforwardly reflects the binding of ANS to hydrophobic regions of the peptide structure. The ANS fluorescence intensity normalized to that at 5 °C shows comparable slopes of temperature dependence for WT and H71A (inset of Fig. 7C). This observation suggests that the thermodynamic properties of ANS binding are not much different between the WT and H71A peptides, and the ANS affinity averaged over individual binding sites does not significantly differ between the two peptides. Accordingly, the ANS fluorescence intensity at a given temperature may be regarded as a measure of the number of ANS biding sites at that temperature.

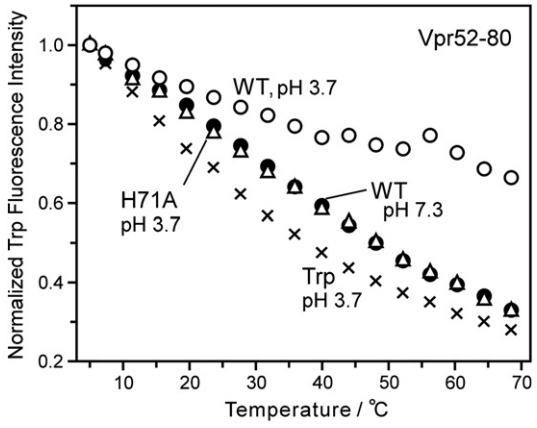

Fig. 6. Temperature dependence of the normalized Trp fluorescence intensity for wild-type Vpr52–80 at pH 3.7 (open circle) and 7.3 (closed circle), the H71A mutant of Vpr52–80 at pH 3.7 (triangle), and amino acid Trp at pH 3.7 (cross). The intensity was normalized to that at 5 °C for each sample.

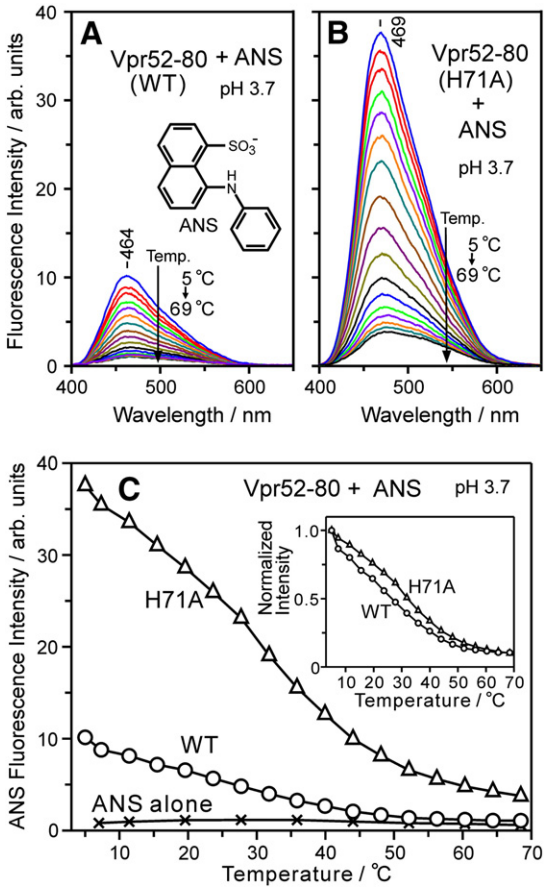

Fig. 7. Fluorescence spectra of ANS in the presence of (A) wild-type Vpr52–80 or (B) its H71A mutant at pH 3.7. The spectra were excited at 370 nm and the temperature was changed from 5 to 69 °C. The peak intensities of ANS fluorescence in the presence of the peptides are plotted against temperature in C (circle for WT and triangle for H71A), where the intensity in the absence of peptide is also plotted for comparison (cross). The inset compares the temperature dependence of the fluorescence intensity normalized to that at 5 °C in the presence of peptide.

The ANS florescence intensity is much weaker for WT Vpr52–80 than for the H71A mutant at every temperature (Fig. 7C), even though the 5-nm blue shift in peak wavelength predicts less polar environment (and stronger fluorescence) for ANS bound to the WT peptide [43]. The unexpectedly large reduction of ANS fluorescence in WT Vpr52–80 compared to the H71A mutant may be explained by a significant decrease of the number of ANS binding sites. Possibly, the His71–Trp54 cation–π interaction, which links both ends of two antiparallel helices of WT Vpr52–80, modifies the mutual arrangement of the helices to a more compact form and prevents ANS molecules from accessing the Leu-zipper-like hydrophobic region in the dimeric interface. The increased compactness of the dimeric structure is consistent with the decreased fluctuation of the Trp54 environment in the presence of His71–Trp54 cation–π interaction (Fig. 6).

4. Discussion

In this study, we have examined the possibility of a cation–π interaction between His71 and Trp54 of the HIV-1 Vpr protein by using the peptide fragment Vpr52–80 containing the H_{III} region, which had been reported to form an antiparallel dimeric interface. Analysis of fluorescence, CD, and UV absorption spectra has revealed that a cation–π interaction occurs between His71 and Trp54 at pH<5.5. The His71–Trp54 cation–π interaction induces a small elongation of the H_{III} helix, an increase in thermal stability of the helical dimer, and a modification of the helical dimer arrangement to produce a more compact dimer. Biological relevance of the present novel findings will be discussed below.

The virion of HIV-1 has been believed to enter host cells through fusion of the viral envelope with the host plasma membrane, followed by uncoating of the viral capsid that covers the viral genomes and proteins including Vpr [2,6]. In that case, Vpr will be released into cytoplasm of the host cell without encountering acidic environments, because the cytoplasmic pH is usually maintained around neutral by homeostasis. However, accumulating evidence indicates that HIV-1 can also enter host cells through endocytosis to initiate productive infection [45–47]. After the endocytosis, the viral genomes and proteins including Vpr will be released within the endosome, whose internal pH can be as low as 5 [48]. Under such acidic conditions, the His71–Trp54 cation–π interaction may occur as revealed here and would affect Vpr-involved processes in an early stage of viral life cycle. In other stages of viral life cycle as well, Vpr is likely to encounter acidic environments. For example, infectious HIV-1 produced by primary macrophages is assembled in late endosomes [49,50], implying a role of the His71–Trp54 cation–π interaction in assembling HIV-1 virions within acidic endosomal compartments.

The pK_a of His71 is 5.5 as described in the Results section. This pK_a value is lower by one pH unit than that of a His residue exposed to solvent water [22]. The lowered pK_a of His71 may be due to nearby positive electric charges that disfavor the protonated cationic state of the imidazole ring of His71. Actually, three positively charged Arg residues are clustered in the C-terminal vicinity of His71 (Arg73, 77, and 80), being consistent with the lowered pK_a value of His71. If the positive charges of the Arg cluster are neutralized by exogenous negative charges, the pK_a of His71 would be raised into a neutral range and the His71–Trp54 cation–π interaction would be possible to take place even at cytoplasmic pH. Vpr binds to a variety of proteins of both viral and host cellular origins [6–9], and the Arg cluster may be involved in such binding through electrostatic interactions with negatively charged regions of target proteins. Mutational studies have shown that Trp54 is essential for Vpr to bind uracil DNA glycosylase, a cellular enzyme involved in base excision repair [51,52], while His71 plays an important role in transport of a viral genome–protein complex containing Vpr itself to the host cell nucleus [53,54]. Although the mechanisms of Vpr binding to such proteins and nucleoproteins are unknown, the pair of Trp54 and His71 may be involved in interactions with viral and cellar components to perform various functions of Vpr.

5. Conclusion

The H_{III} region of HIV-1 Vpr protein forms an antiparallel helical dimer not only at acidic pH reported previously but also at neutral pH. Upon protonation of His71 at pH<5.5, a cation–π interaction occurs between His71 and Trp54 belonging to different H_{III} helices. The cation–π interaction plays a role in stabilizing and tuning the dimeric structure of Vpr, at least in the H_{III} region. Vpr may utilize the His71–Trp54 cation–π interaction to achieve its proper interactions with various kinds of viral and cellular components. The structural modification by the cation–π interaction is one of the novel findings of this study and is expected to serve as a clue to structural understanding of the roles of Vpr in the virus life cycle and in the pathogenesis of AIDS.

Acknowledgment

This work was supported in part by a Grant-in-Aid for Scientific Research (B) (23390008) from the Japan Society for the Promotion of Science.

References

[1] K.A. Sepkowitz, AIDS—the first 20 years, The New England Journal of Medicine 344 (2001) 1764–1772.
[2] J.M. Costin, Cytopathic mechanisms of HIV-1, Virology Journal 4 (2007) 100.
[3] M.H. Malim, M. Emerman, HIV-1 accessory proteins—ensuring viral survival in a hostile environment, Cell Host & Microbe 3 (2008) 388–398.
[4] T. Gramberg, N. Sunseri, N.R. Landau, Accessories to the crime: recent advances in HIV accessory protein biology, Current HIV/AIDS Reports 6 (2009) 36–42.
[5] B. Romani, S. Engelbrecht, Human immunodeficiency virus type 1 Vpr: functions and molecular interactions, Journal of General Virology 90 (2009) 1795–1805.
[6] R.Y. Zhao, G. Li, M.I. Bukrinsky, Vpr-host interactions during HIV-1 viral life cycle, Journal of Neuroimmune Pharmacology 6 (2011) 216–229.
[7] M. Kogan, J. Rappaport, HIV-1 accessory protein Vpr: relevance in the pathogenesis of HIV and potential for therapeutic intervention, Retrovirology 8 (2011) 25.
[8] N. Morellet, B.P. Roques, S. Bouaziz, Structure–function relationship of Vpr: biological implications, Current HIV Research 7 (2009) 184–210.
[9] R.C. Pandey, D. Datta, R. Mukerjee, A. Srinivasan, S. Mahalingam, B.E. Sawaya, HIV-1 Vpr: a closer look at the multifunctional protein from the structural perspective, Current HIV Research 7 (2009) 114–128.
[10] K. Ogawa, R. Shibata, T. Kiyomasu, I. Higuchi, Y. Kishida, A. Ishimoto, A. Adachi, Mutational analysis of the human immunodeficiency virus vpr open reading frame, Journal of Virology 63 (1989) 4110–4114.
[11] E.A. Cohen, E.F. Terwilliger, Y. Jalinoos, J. Proulx, J.G. Sodroski, W.A. Haseltine, Identification of HIV-1 vpr product and function, Journal of Acquired Immune Deficiency Syndromes 3 (1990) 11–18.
[12] K. Wecker, B.P. Roques, NMR structure of the (1–51) N-terminal domain of the HIV-1 regulatory protein, Vpr, European Journal of Biochemistry 266 (1999) 359–369.
[13] W. Schüler, K. Wecker, H. de Rocquigny, Y. Baudat, J. Sire, B.P. Roques, NMR structure of the (52–96) C-terminal domain of the HIV-1 regulatory protein Vpr: molecular insights into its biological functions, Journal of Molecular Biology 285 (1999) 2105–2117.
[14] A. Engler, T. Stangler, D. Willbold, Solution structure of human immunodeficiency virus type 1 Vpr(13–33) peptide in micelles, European Journal of Biochemistry 268 (2001) 389–395.
[15] A. Engler, T. Stangler, D. Willbold, Structure of human immunodeficiency virus type 1 Vpr(34–51) peptide in micelle containing aqueous solution, European Journal of Biochemistry 269 (2002) 3264–3269.
[16] K. Wecker, N. Morellet, S. Bouaziz, B.P. Roques, NMR structure of the HIV-1 regulatory protein Vpr in H_2O/trifluoroethanol. Comparison with the Vpr N-terminal (1–51) and C-terminal (52–96) domains, European Journal of Biochemistry 269 (2002) 3779–3788.
[17] N. Morellet, S. Bouaziz, P. Petitjean, B.P. Roques, NMR structure of the HIV-1 regulatory protein VPR, Journal of Molecular Biology 327 (2003) 215–227.
[18] K. Bruns, T. Fossen, V. Wray, P. Henklein, U. Tessmer, U. Schubert, Structural characterization of the HIV-1 Vpr N terminus: evidence of cis/trans-proline isomerism, Journal of Biological Chemistry 278 (2003) 43188–43201.
[19] S. Bourbigot, H. Beltz, J. Denis, N. Morellet, B.P. Roques, Y. Mély, S. Bouaziz, The C-terminal domain of the HIV-1 regulatory protein Vpr adopts an antiparallel dimeric structure in solution via its leucine-zipper-like domain, Biochemical Journal 387 (2005) 333–341.
[20] B. Romani, R. Glashoff, S. Engelbrecht, Molecular and phylogenetic analysis of HIV type 1 vpr sequences of South African strains, AIDS Research and Human Retroviruses 25 (2009) 357–362.
[21] B. Romani, R.H. Glashoff, S. Engelbrecht, Functional integrity of naturally occurring mutants of HIV-1 subtype C Vpr, Virus Research 153 (2010) 288–298.

[22] G.R. Grimsley, J.M. Scholtz, C.N. Pace, A summary of the measured pK values of the ionizable groups in folded proteins, Protein Science 18 (2009) 247–251.
[23] D.A. Dougherty, Cation–π interactions in chemistry and biology: a new view of benzene, Phe, Tyr, and Trp, Science 271 (1996) 163–168.
[24] J.C. Ma, D.A. Dougherty, The cation–π interaction, Chemical Reviews 97 (1997) 1303–1324.
[25] A. Okada, T. Miura, H. Takeuchi, Protonation of histidine and histidine–tryptophan interaction in the activation of the M2 ion channel from influenza a virus, Biochemistry 40 (2001) 6053–6060.
[26] Y. Xue, A.V. Davis, G. Balakrishnan, J.P. Stasser, B.M. Staehlin, P. Focia, T.G. Spiro, J.E. Penner-Hahn, T.V. O'Halloran, Cu(I) recognition via cation–π and methionine interactions in CusF, Nature Chemical Biology 4 (2008) 107–109.
[27] H. Yorita, K. Otomo, H. Hiramatsu, A. Toyama, T. Miura, H. Takeuchi, Evidence for the cation–π interaction between Cu_2^+ and tryptophan, Journal of the American Chemical Society 130 (2008) 15266–15267.
[28] J.V. Fritz, P. Didier, J.P. Clamme, E. Schaub, D. Muriaux, C. Cabanne, N. Morellet, S. Bouaziz, J.L. Darlix, Y. Mély, H. de Rocquigny, Direct Vpr–Vpr interaction in cells monitored by two photon fluorescence correlation spectroscopy and fluorescence lifetime imaging, Retrovirology 5 (2008) 87.
[29] N.J. Venkatachari, L.A. Walker, O. Tastan, T. Le, T.M. Dempsey, Y. Li, N. Yanamala, A. Srinivasan, J. Klein-Seetharaman, R.C. Montelaro, V. Ayyavoo, Human immunodeficiency virus type 1 Vpr: oligomerization is an essential feature for its incorporation into virus particles, Virology Journal 7 (2010) 119.
[30] M. Cardamone, N.K. Puri, Spectrofluorimetric assessment of the surface hydrophobicity of proteins, Biochemical Journal 282 (1992) 589–593.
[31] W.R. Kirk, E. Kurian, F.G. Prendergast, Characterization of the sources of protein-ligand affinity: 1-sulfonato-8-(1′)anilinonaphthalene binding to intestinal fatty acid binding protein, Biophysical Journal 70 (1996) 69–83.
[32] C.N. Pace, F. Vajdos, L. Fee, G. Grimsley, T. Gray, How to measure and predict the molar absorption coefficient of a protein, Protein Science 4 (1995) 2411–2423.
[33] N. Sreerama, R.W. Woody, Estimation of protein secondary structure from circular dichroism spectra: comparison of CONTIN, SELCON, and CDSSTR methods with an expanded reference set, Analytical Biochemistry 287 (2000) 252–260.
[34] A.S. Ladokhin, Encyclopedia of analytical chemistry, in: R.A. Meyers (Ed.), Fluorescence Spectroscopy in Peptide and Protein Analysis, John Wiley and Sons, Chichester, 2000, p. 5762.
[35] J.N. Weiss, The Hill equation revisited: uses and misuses, The FASEB Journal 11 (1997) 835–841.
[36] R. Loewenthal, J. Sancho, A.R. Fersht, Fluorescence spectrum of barnase: contributions of three tryptophan residues and a histidine-related pH dependence, Biochemistry 30 (1991) 6775–6779.
[37] R. Vos, Y. Engelborghs, A fluorescence study of tryptophan-histidine interactions in the peptide anantin and in solution, Photochemistry and Photobiology 60 (1994) 24–32.
[38] J.R. Lakowicz, Principles of Fluorescence Spectroscopy, Springer, New York, 2006.
[39] K. Rosenheck, P. Doty, The far ultraviolet absorption spectra of polypeptide and protein solutions and their dependence on conformation, Proceedings of the National Academy of Sciences of the United 47 (1961) 1775–1785.
[40] L.G.M. Baas Becking, On the analysis of sigmoid curves, Acta Biotheoretica 8 (1946) 42–59.
[41] J.R. Albani, Principles and Applications of Fluorescence Spectroscopy, Blackwell, Oxford, 2007.
[42] T.L. Bushueva, E.P. Busel, E.A. Burstein, Relationship of thermal quenching of protein fluorescence to intramolecular structural mobility, Biochimica et Biophysica Acta 34 (1978) 141–152.
[43] A. Hawe, M. Sutter, W. Jiskoot, Extrinsic fluorescent dyes as tools for protein characterization, Pharmaceutical Research 25 (2008) 1487–1499.
[44] D. Matulis, R. Lovrien, 1-Anilino-8-naphthalene sulfonate anion–protein binding depends primarily on ion pair formation, Biophysical Journal 74 (1998) 422–429.
[45] K. Miyauchi, Y. Kim, O. Latinovic, V. Morozov, G.B. Melikyan, HIV enters cells via endocytosis and dynamin-dependent fusion with endosomes, Cell 137 (2009) 433–444.
[46] K. Miyauchi, M. Marin, G.B. Melikyan, Visualization of retrovirus uptake and delivery into acidic endosomes, Biochemical Journal 434 (2011) 559–569.
[47] K. Pritschet, N. Donhauser, P. Schuster, M. Ries, S. Haupt, N.A. Kittan, K. Korn, S. Pöhlmann, G. Holland, N. Bannert, E. Bogner, B. Schmidt, CD4- and dynamin-dependent endocytosis of HIV-1 into plasmacytoid dendritic cells, Virology 423 (2012) 152–164.
[48] I. Mellman, R. Fuchs, A. Helenius, Acidification of the endocytic and exocytic pathways, Annual Review of Biochemistry 55 (1986) 663–700.
[49] A. Pelchen-Matthews, B. Kramer, M. Marsh, Infectious HIV-1 assembles in late endosomes in primary macrophages, The Journal of Cell Biology 162 (2003) 443–455.
[50] P. Benaroch, E. Billard, R. Gaudin, M. Schindler, M. Jouve, HIV-1 assembly in macrophages, Retrovirology 7 (2010) 29.
[51] L. Selig, S. Benichou, M.E. Rogel, L.I. Wu, M.A. Vodicka, J. Sire, R. Benarous, M. Emerman, Uracil DNA glycosylase specifically interacts with Vpr of both human immunodeficiency virus type 1 and simian immunodeficiency virus of sooty mangabeys, but binding does not correlate with cell cycle arrest, Journal of Virology 71 (1997) 4842–4846.
[52] L.M. Mansky, S. Preveral, L. Selig, R. Benarous, S. Benichou, The interaction of Vpr with uracil DNA glycosylase modulates the human immunodeficiency virus type 1 in vivo mutation rate, Journal of Virology 74 (2000) 7039–7047.
[53] S. Mahalingam, R.G. Collman, M. Patel, C.E. Monken, A. Srinivasan, Functional analysis of HIV-1 Vpr: identification of determinants essential for subcellular localization, Virology 212 (1995) 331–339.
[54] M.A. Vodicka, D.M. Koepp, P.A. Silver, M. Emerman, HIV-1 Vpr interacts with the nuclear transport pathway to promote macrophage infection, Genes & Development 12 (1998) 175–185.